Supporting Information

Low-cost porous organic polymer based on aromatic ketones for photocatalytic oxygen activation and H_2O_2 production

Yinwei Wang,[a,b] Shuang Li,[a] Xiao Feng,[a,b] Jin Gao,*[a] and Song Shi*[a]

[a] Y. Wang, S. Li, X. Feng, Dr. J. Gao, Dr. S. Shi
State Key Laboratory of Catalysis, Dalian National Laboratory for Clean Energy, Dalian Institute of Chemical Physics, Chinese Academy of Sciences
457 Zhongshan Road, Dalian 116023 (P. R. China)
[b] Y. Wang, X. Feng
University of Chinese Academy of Sciences
Beijing 100049 (P. R. China)

*Corresponding authors:
E-mail address: shisong@dicp.ac.cn (S. Shi); E-mail: gaojin@dicp.ac.cn (J. Gao).

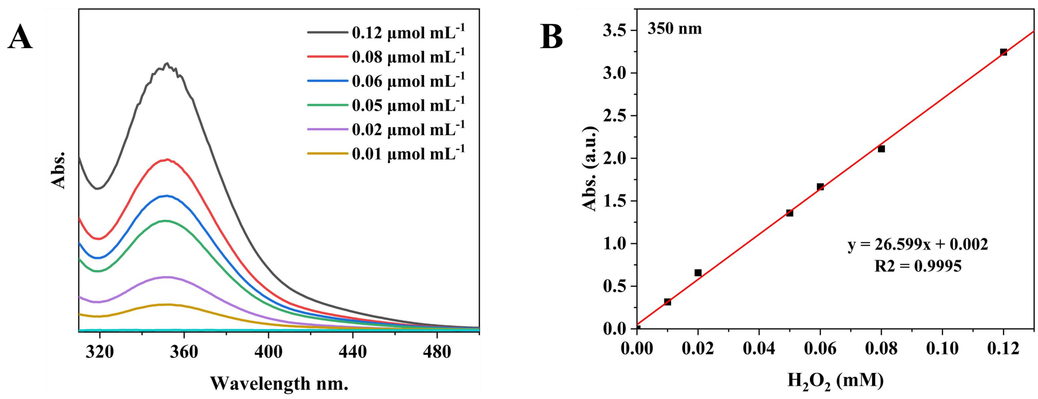

Figure S1. Quantitative detection of H_2O_2. (A) UV-vis absorption spectra of different concentrations of H_2O_2 under iodometry; (B) Standard curves for quantitative detection of H_2O_2.

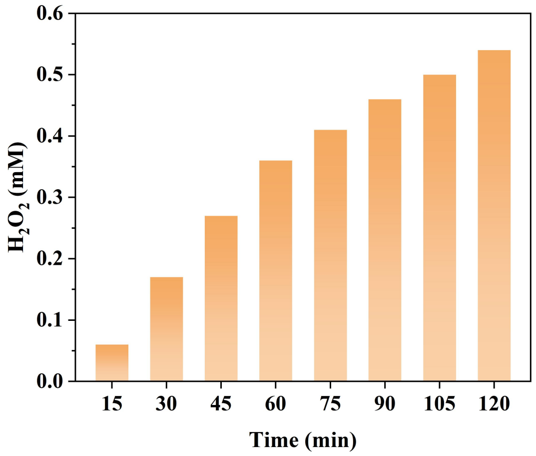

Figure S2. Changes of H_2O_2 concentration over time under TPN-CO-Eth catalysis.

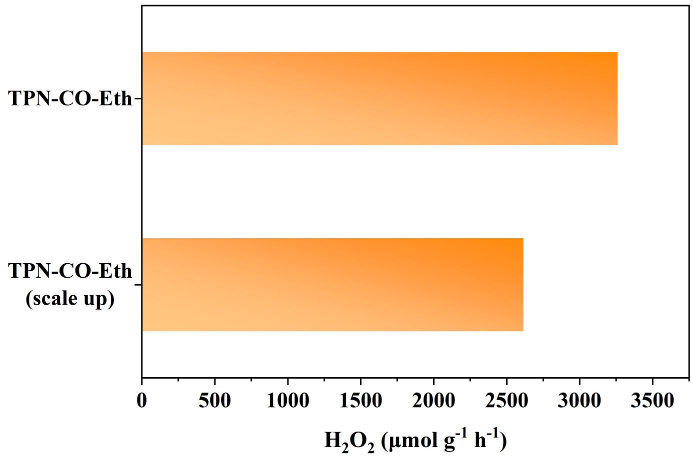

Figure S3. Comparison of photocatalytic H_2O_2 production rates of TPN-CO-Eth and TPN-CO-Eth (scale-up).

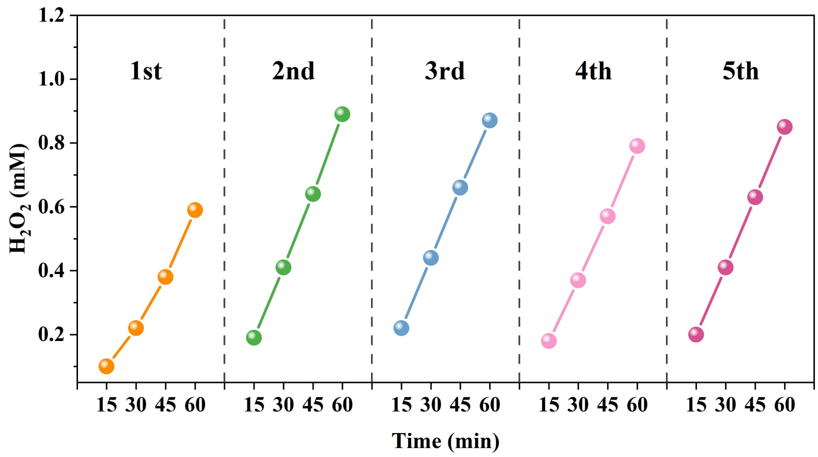

Figure S4. The recyclability of TPN-CO-Eth.

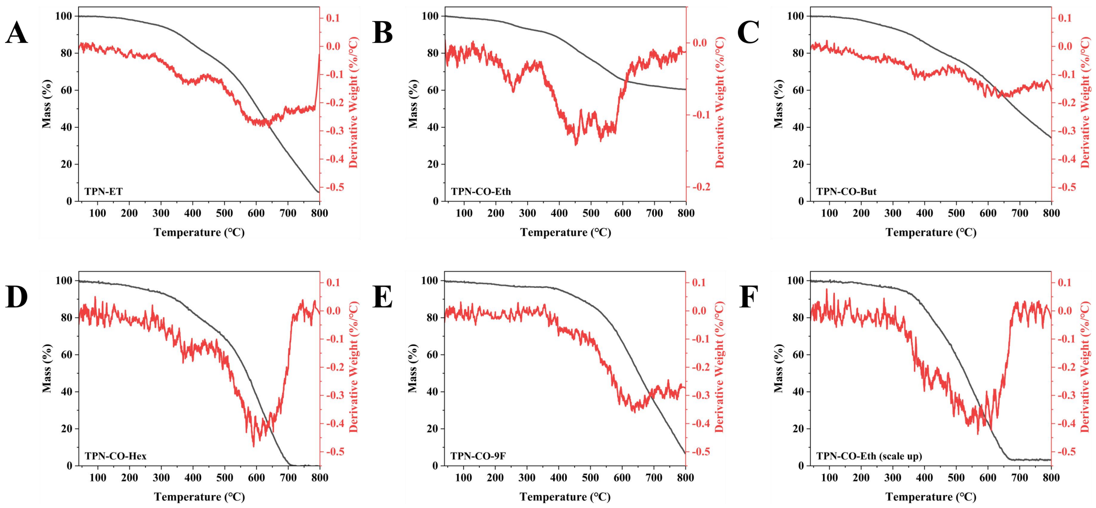

Figure S5. Thermogravimetric and derivative thermogravimetric analysis of the catalysts. (A) TPN-ET; (B) TPN-CO-Eth; (C) TPN-CO-But; (D) TPN-CO-Hex; (E) TPN-CO-9F; (F) TPN-CO-Eth (scale-up).

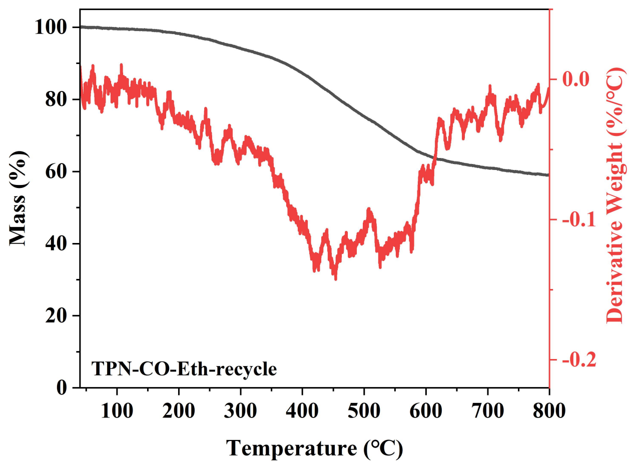

Figure S6. Thermogravimetric and derivative thermogravimetric analysis of the recycled TPN-CO-Eth.

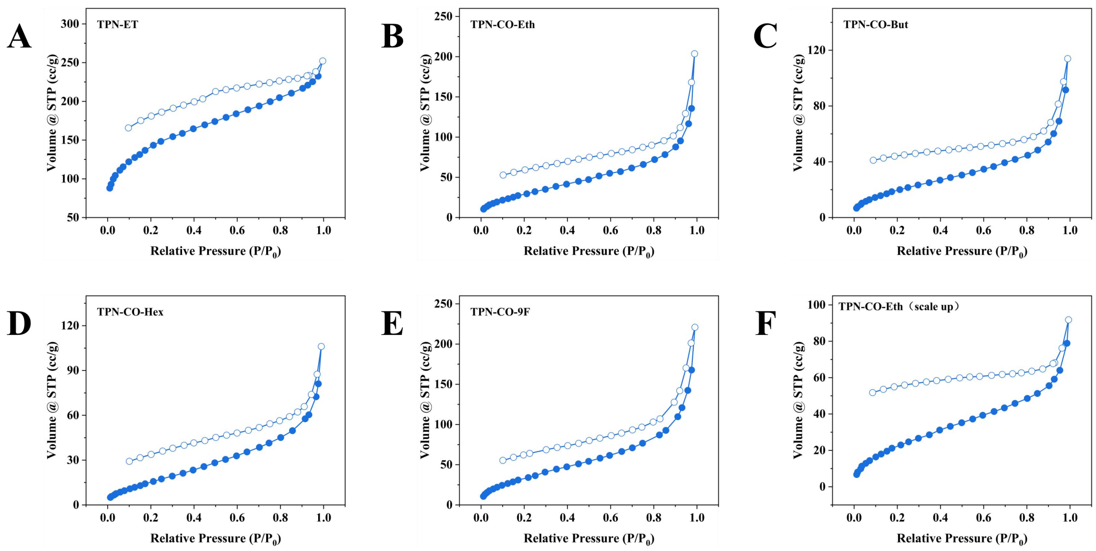

Figure S7. Nitrogen adsorption-desorption isotherm of the catalysts. (A) TPN-ET; (B) TPN-CO-Eth; (C) TPN-CO-But; (D) TPN-CO-Hex; (E) TPN-CO-9F; (F) TPN-CO-Eth (scale-up).

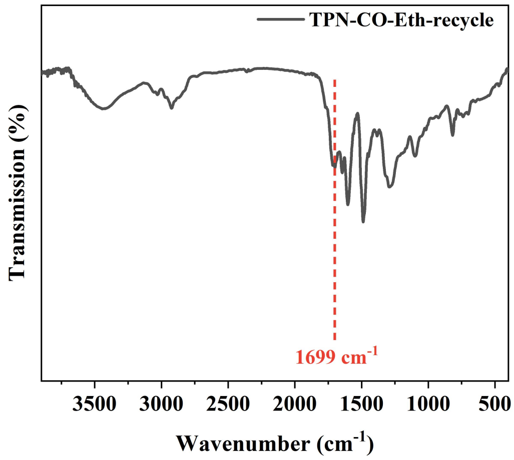

Figure S8. FT-IR spectra of the recycled TPN-CO-Eth.

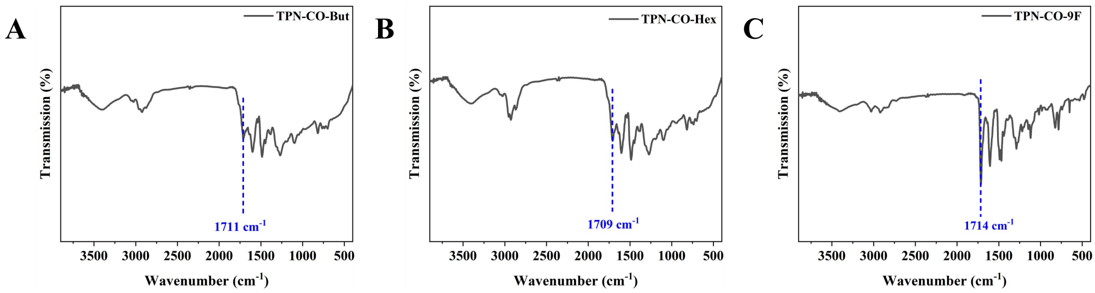

Figure S9. FT-IR spectra of catalysts. (A) TPN-CO-But, (B) TPN-CO-Hex, and (C) TPN-CO-9F.

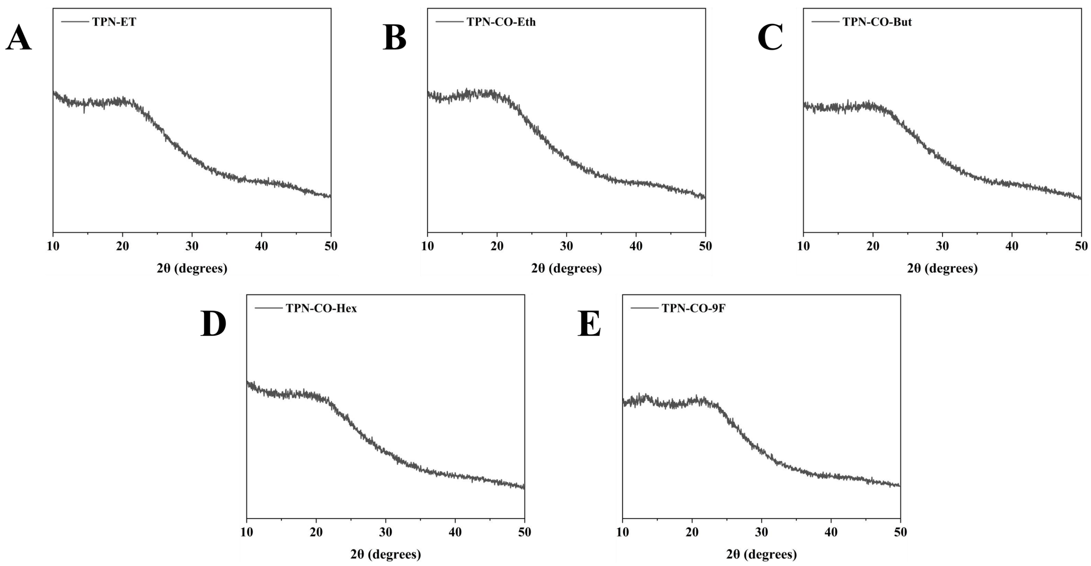

Figure S10. XRD spectrum of the catalysts. (A) TPN-ET; (B) TPN-CO-Eth; (C) TPN-CO-But; (D) TPN-CO-Hex; (E) TPN-CO-9F.

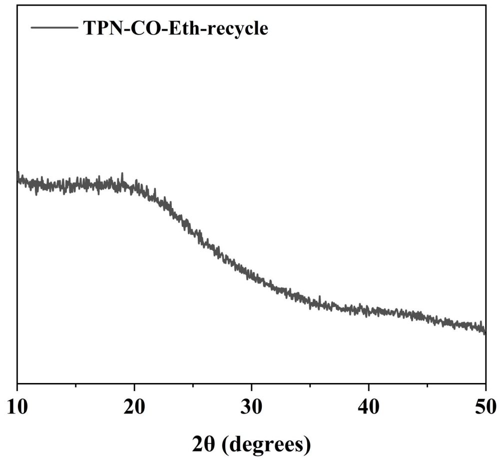

Figure S11. XRDspectrum of the recycled TPN-CO-Eth.

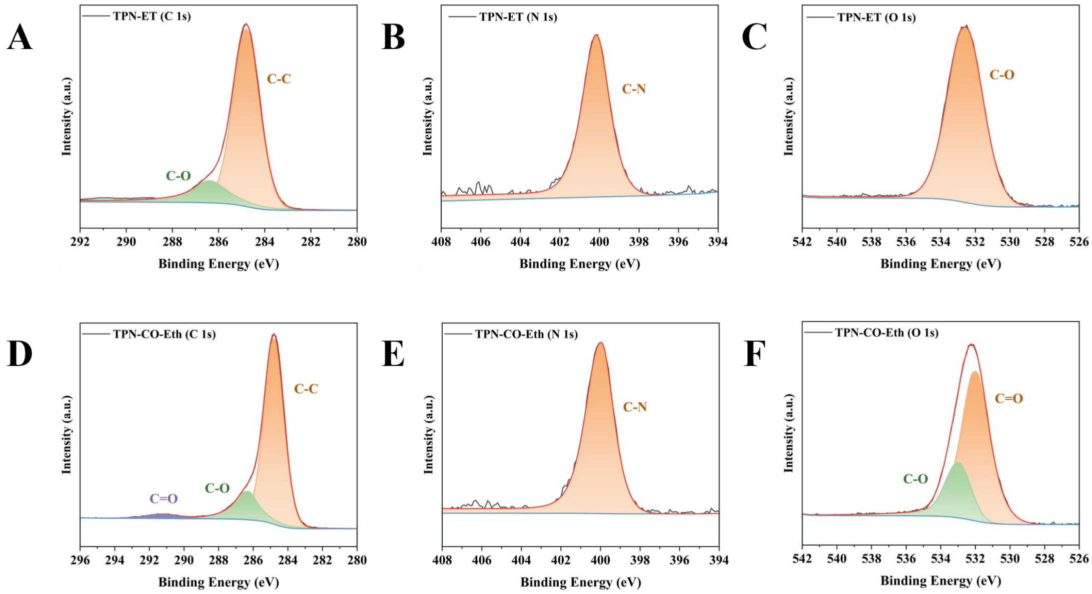

Figure S12. XPS spectrum of catalysts. (A) C 1s, (B) N 1s and (C) O 1s XPS spectra of TPN-ET; (D) C 1s, (E) N 1s and (F) O 1s XPS spectra of TPN-CO-Eth.

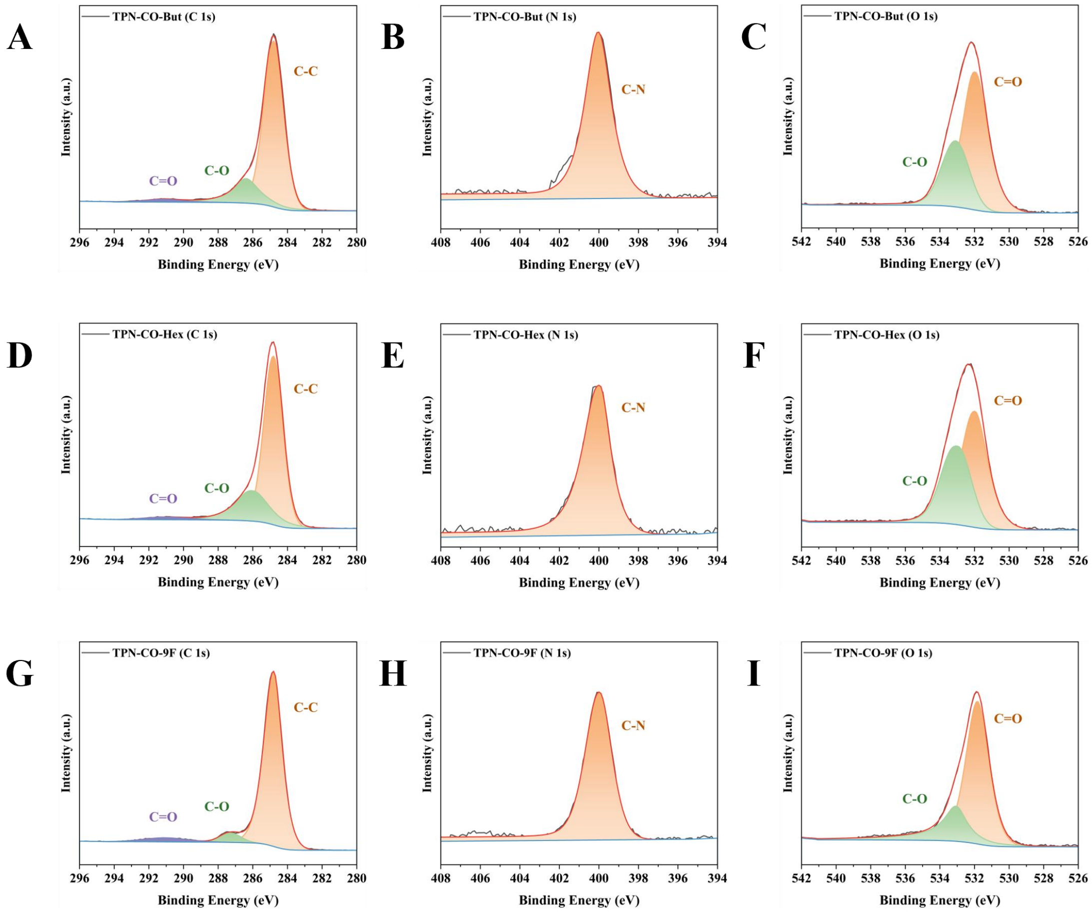

Figure S13. XPS spectrum of catalysts. (A) C 1s, (B) N 1s and (C) O 1s XPS spectra of TPN-CO-But; (D) C 1s, (E) N 1s and (F) O 1s XPS spectra of TPN-CO-Hex; (G) C 1s, (H) N 1s and (I) O 1s XPS spectra of TPN-CO-9F.

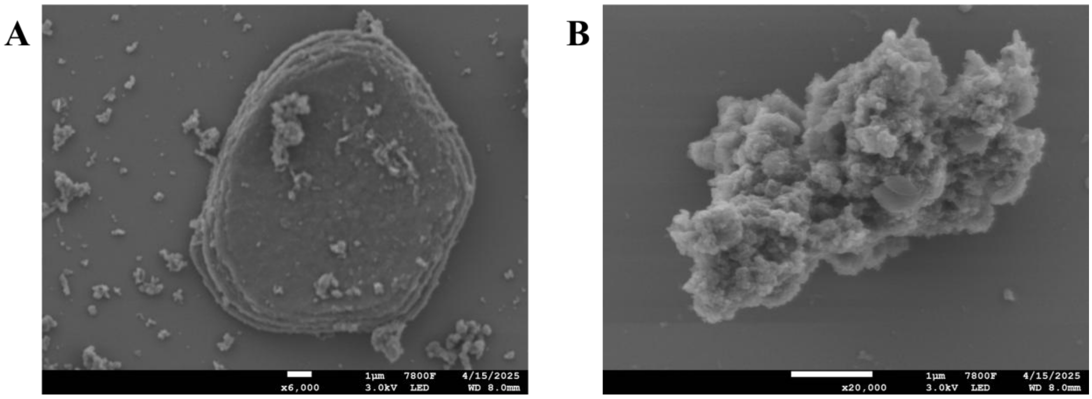

Figure S14. SEM image of the catalysts. (A) TPN-CO-Eth; (B) TPN-ET.

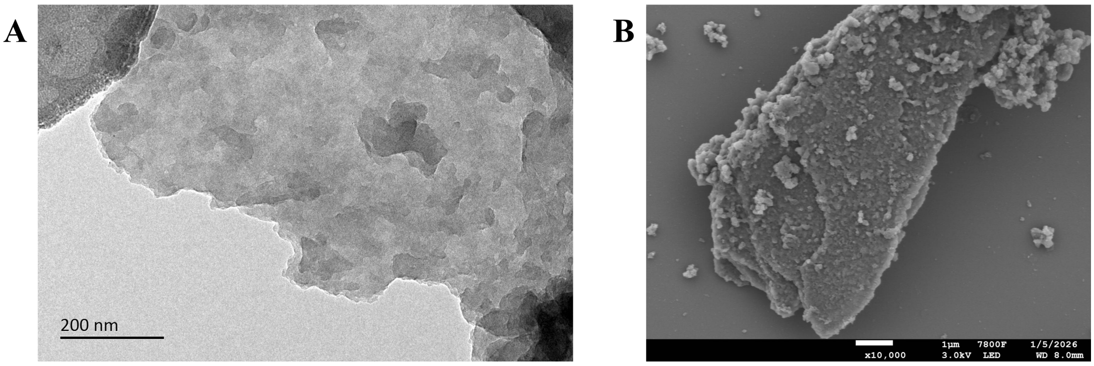

Figure S15. Morphology of the recycled TPN-CO-Eth. (A) HR-TEM image and (B) SEM image.

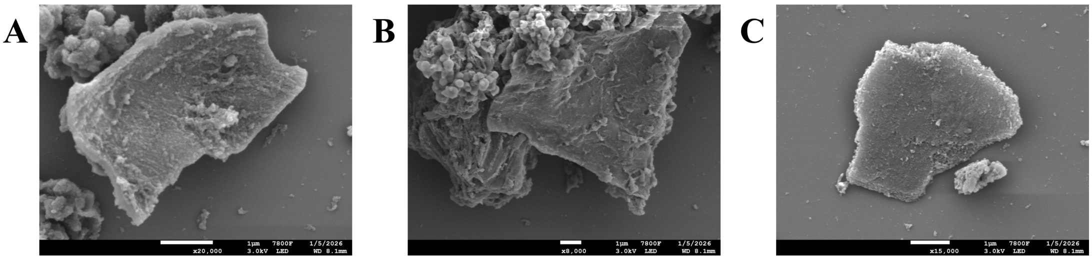

Figure S16. SEM image of the catalysts. (A) TPN-CO-But; (B) TPN-CO-Hex; (C) TPN-CO-9F.

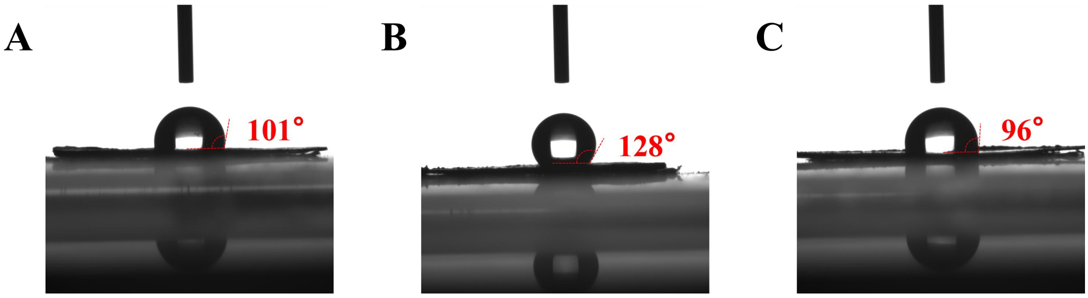

Figure S17. The contact angle of catalysts. (A) TPN-CO-But; (B) TPN-CO-Hex; (C) TPN-CO-9F.

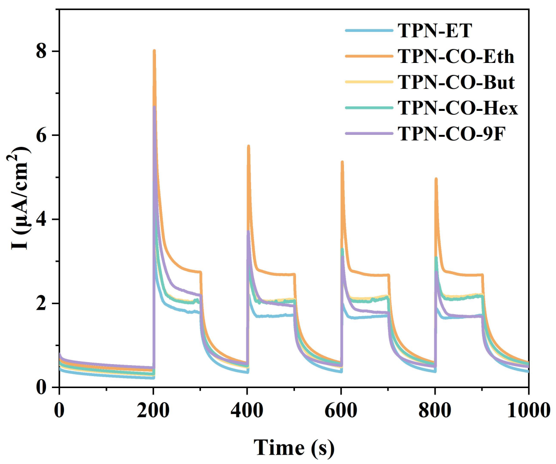

Figure S18. Photocurrent response performance of TPN-ET, TPN-CO-Eth, TPN-CO-But, TPN-CO-Hex, and TPN-CO-9F.

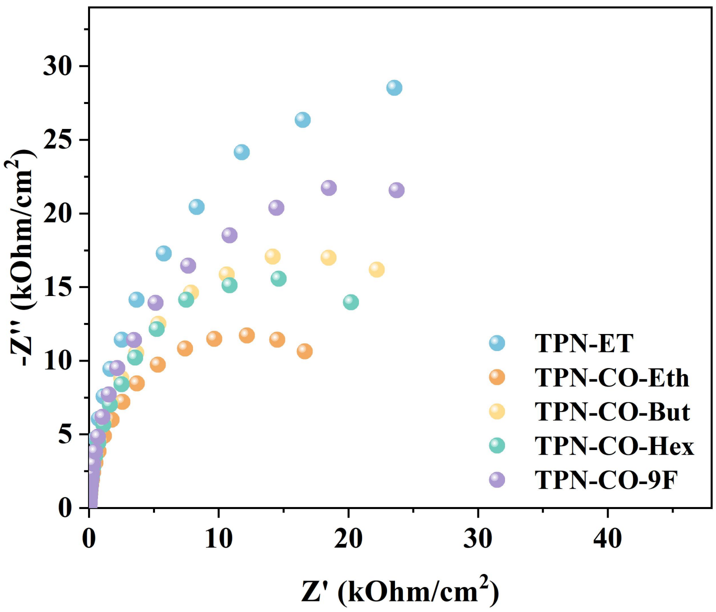

Figure S19. EIS spectra of TPN-ET, TPN-CO-Eth, TPN-CO-But, TPN-CO-Hex, and TPN-CO-9F.

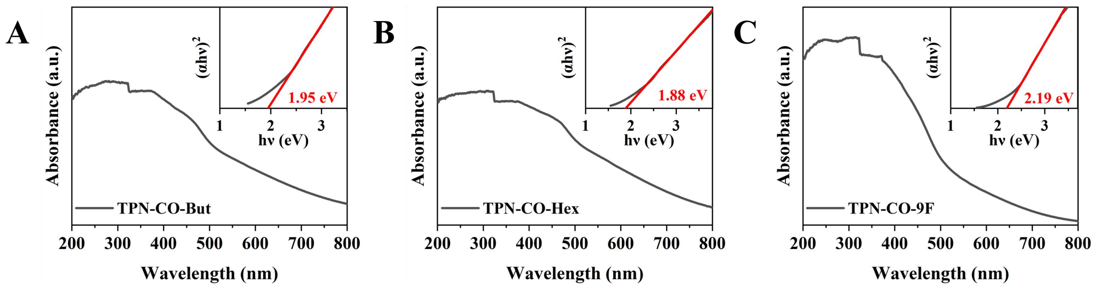

Figure S20. UV-vis DRS spectra (the inset figure is the Tauc plot) of catalysts. (A) TPN-CO-But, (B) TPN-CO-Hex, and (C) TPN-CO-9F.

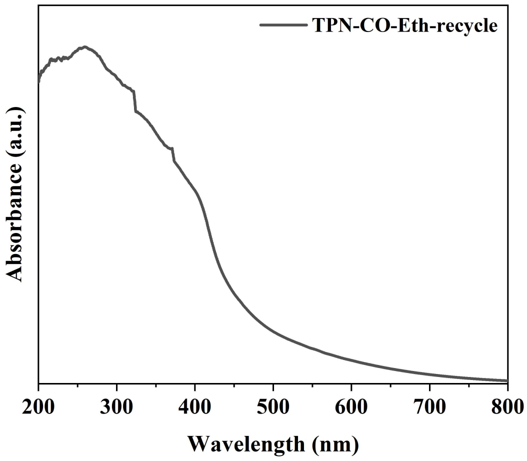

Figure S21. UV-vis DRS spectra of the recycled TPN-CO-Eth.

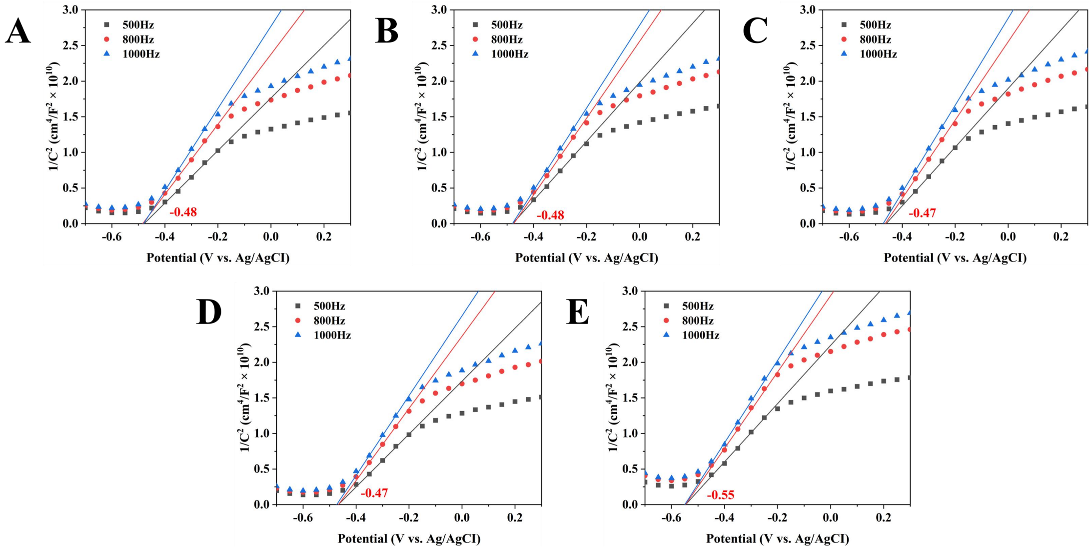

Figure S22. Mott-Schottky plots of the catalysts. (A) TPN-ET; (B) TPN-CO-Eth; (C) TPN-CO-But; (D) TPN-CO-Hex; (E) TPN-CO-9F.

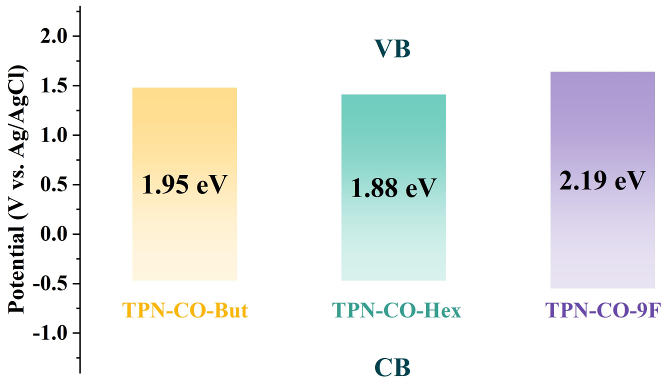

Figure S23. Band structure of TPN-CO-But, TPN-CO-Hex, and TPN-CO-9F.

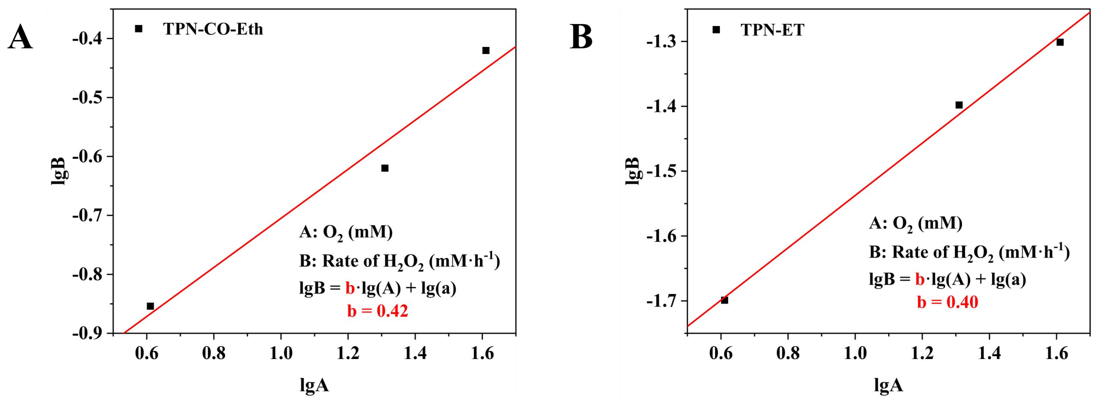

Figure S24. Reaction order of oxygen on the catalysts. (A) TPN-CO-Eth; (B) TPN-ET.

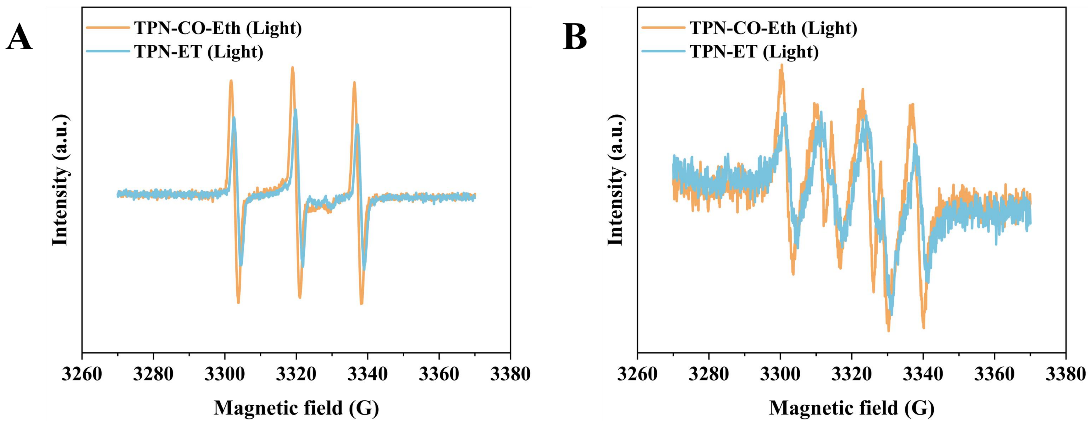

Figure S25. EPR spectra. Comparison of EPR spectra of (A) TEMP-$^1O_2$ and (B) DMPO-$\cdot O_2^-$ radical trapping experiments catalyzed by TPN-CO-Eth and TPN-ET.

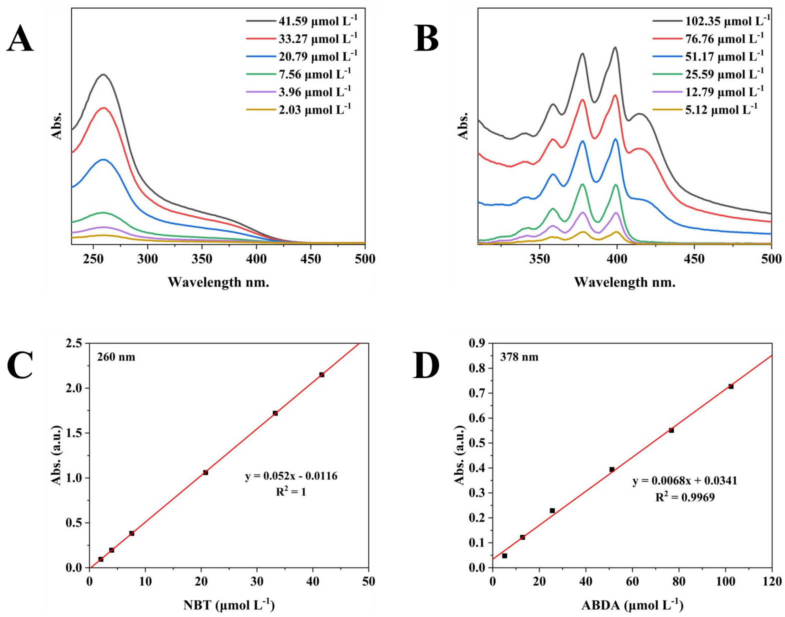

Figure S26. Quantitative detection of NBT and ABDA. UV-vis absorption spectra of different concentrations of (A) NBT and (B) ABDA; Standard curves for quantitative detection of (C) NBT and (D) ABDA.

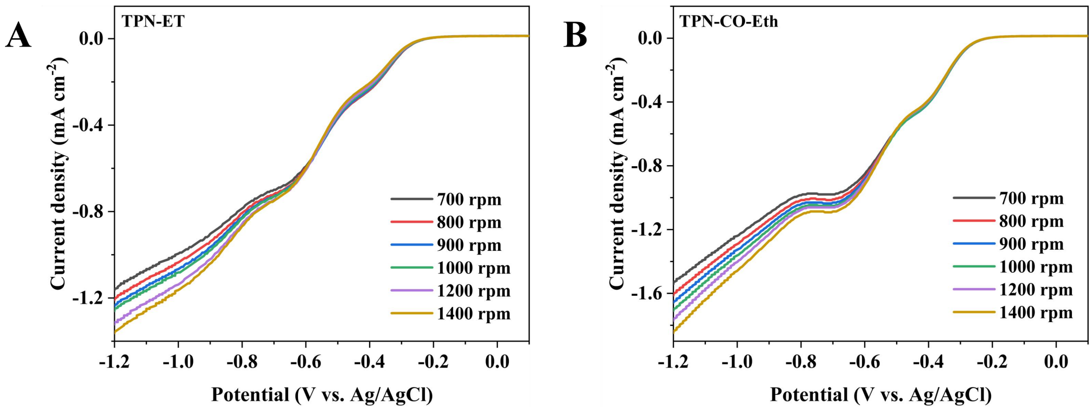

Figure S27. Linear-sweep RDE voltammograms of catalysts at different rotating speeds. (A) TPN-ET, (B) TPN-CO-Eth.

Table S1. The comparison of the photocatalytic H_2O_2 production rate of organic polymer-based catalysts in pure water.

Catalyst	Atmosphere	Irradiation condition	H_2O_2 yield (μmol g^{-1} h^{-1})	Ref.
TPN-CO-Eth	O_2	20 W LED light (455-460 nm)	3798	This work
TTP-1	Air	300 W Xe lamp (λ > 420 nm)	3132	[1]
sp2c-CTF-4@AB	O_2	40 W blue LED (λ > 420 nm)	2758	[2]
NMP	Air	300 W Xe lamp (AM 1.5G)	2552.5	[3]
CTF-FL	O_2	300 W Xe lamp (λ > 420 nm)	2412.1	[4]
Post-v-COF-F2	O_2	40 W blue LED (455 nm)	2219	[5]
HCOF	O_2	300 W Xe lamp (λ > 420 nm)	2113.9	[6]
BTDB-CN0.2	Air	300 W Xe lamp (λ > 420 nm)	1920	[7]
HEP-TAPT-COF	O_2	300 W Xe lamp (λ > 420 nm)	1750	[8]
COF-2CN	O_2	300 W Xe lamp (λ > 420 nm)	1601	[9]
BTT-H2 COF	O_2	40 W blue LED (467 nm)	1588	[10]
COF-TPT-Azo	O_2	300 W Xe lamp (λ > 420 nm)	1498	[11]
FS-OHOMe-COF	Air	300 W Xe lamp (λ > 420 nm)	1480	[12]
PMCR-1	O_2	300 W Xe lamp (λ > 420 nm)	1445	[13]
TpaBtt-COF	O_2	300 W Xe lamp (λ > 420 nm)	1407	[14]
CTF-TD	O_2	300 W Xe lamp (λ > 420 nm)	1342	[15]
TDB-COF	O_2	300 W Xe lamp (AM 1.5G)	723.5	[16]
COF-TfpBpy	O_2	300 W Xe lamp (λ > 420 nm)	695	[17]
COF-N32	O_2	300 W Xe lamp (λ > 420 nm)	605	[18]
TpAQ-COF-12	O_2	300 W Xe lamp (λ > 420 nm)	420	[19]
TZ-COF	O_2	300 W Xe lamp (λ > 420 nm)	268	[20]

References

[1] C. C. Chu, Z. Chen, D. C. Yao, X. R. Liu, M. J. Cai, S. Mao, Large-Scale Continuous and In Situ Photosynthesis of Hydrogen Peroxide by Sulfur-Functionalized Polymer Catalyst for Water Treatment, Angew. Chem. Int. Ed. 63 (2024) e202317214.

[2] Q. J. Xie, A. Q. Chen, X. F. Li, C. Xu, S. Bi, W. J. Zhang, J. T. Tang, C. Y. Pan, F. Zhang, G. P. Yu, Tuning the interlayer stacking of a vinylene-linked covalent organic framework for enhancing sacrificial agent-free hydrogen peroxide photoproduction, Chem. Sci. 16 (2025) 2215-2221.

[3] C. Yang, Y. Xiang, W. Wang, B. Cheng, K. Yang, J. G. Yu, S. W. Cao, Enhancing photocatalytic H_2O_2 production of donor-acceptor polymers by modulation of polymerization modes, Appl. Catal. B Environ. 365 (2025) 124856.

[4] L. Zhang, C. X. Wang, Q. K. Jiang, P. B. Lyu, Y. X. Xu, Structurally Locked High-Crystalline Covalent Triazine Frameworks Enable Remarkable Overall Photosynthesis of Hydrogen Peroxide, J. Am. Chem. Soc. 146 (2024) 29943-29954.

[5] A. Q. Chen, Y. Jian, Q. J. Xie, W. Li, C. Y. Pan, G. P. Yu, S. Gu, J. T. Tang, End-capping fluorination of vinylene-linked covalent organic frameworks for photocatalytic hydrogen peroxide production, Chem. Commun. 61 (2025) 7101-7104.

[6] Q. Zhu, L. Shi, Z. Li, G. S. Li, X. X. Xu, Protonation of an Imine-linked Covalent Organic Framework for Efficient H_2O_2 Photosynthesis under Visible Light up to 700 nm, Angew. Chem. Int. Ed. 63 (2024) e202408041.

[7] J. Z. Cheng, W. Wang, J. J. Zhang, S. J. Wan, B. Cheng, J. G. Yu, S. W. Cao, Molecularly Tunable Heterostructured Co-Polymers Containing Electron-Deficient and -Rich Moieties for Visible-Light and Sacrificial-Agent-Free H_2O_2 Photosynthesis, Angew. Chem. Int. Ed. 63 (2024) e202406310.

[8] D. Chen, W. B. Chen, Y. T. Wu, L. Wang, X. J. Wu, H. X. Xu, L. Chen, Covalent Organic Frameworks Containing Dual O_2 Reduction Centers for Overall Photosynthetic Hydrogen Peroxide Production, Angew. Chem. Int. Ed. 62 (2023) e202217479.

[9] Y. H. Hou, P. Zhou, F. Y. Liu, Y. Y. Lu, H. Tan, Z. M. Li, M. P. Tong, J. R. Ni, Efficient Photosynthesis of Hydrogen Peroxide by Cyano-Containing Covalent Organic Frameworks from Water, Air and Sunlight, Angew. Chem. Int. Ed. 63 (2024) e202318562.

[10] A. Chakraborty, A. Alam, U. Pal, A. Sinha, S. Das, T. Saha-Dasgupta, P. Pachfule, Enhancing photocatalytic hydrogen peroxide generation by tuning hydrazone linkage density in covalent organic frameworks, Nat. Commun. 16 (2025) 503.

[11] H. H. Sun, Z. B. Zhou, Y. B. Fu, Q. Y. Qi, Z. X. Wang, S. Q. Xu, X. Zhao, Azobenzene-Bridged Covalent Organic Frameworks Boosting Photocatalytic Hydrogen Peroxide Production from Alkaline Water: One Atom Makes a Significant Improvement, Angew. Chem. Int. Ed. 63 (2024) e202409250.

[12] C. Shu, X. J. Yang, L. J. Liu, X. L. Hu, R. X. Sun, X. Yang, A. I. Cooper, B. Tan, X. Y. Wang, Mixed-Linker Strategy for the Construction of Sulfone-Containing D-A-A Covalent Organic Frameworks for Efficient Photocatalytic Hydrogen Peroxide Production, Angew. Chem. Int. Ed. 63 (2024) e202403926.

[13] P. Das, J. Roeser, A. Thomas, Solar Light Driven H_2O_2 Production and Selective Oxidations Using a Covalent Organic Framework Photocatalyst Prepared by a Multicomponent Reaction, Angew. Chem. Int. Ed. 62 (2023) e202304349.

[14] C. C. Qin, X. D. Wu, L. Tang, X. H. Chen, M. Li, Y. Mou, B. Su, S. B. Wang, C. Y. Feng, J. W. Liu, X. Z. Yuan, Y. L. Zhao, H. Wang, Dual donor-acceptor covalent organic frameworks for hydrogen peroxide photosynthesis, Nat. Commun. 14 (2023) 5238.
[15] Q. H. Zhang, J. Y. Zhou, H. N. Zhang, C. Qi, Q. Zhou, R. Z. Guo, H. Yang, T. Xing, M. Q. Wang, M. B. Wu, W. T. Wu, Terphenyl Functionalized Covalent Triazine Polymer as Metal-Free Photocatalyst for Superior Hydrogen Peroxide Production, Adv. Funct. Mater. 34 (2024) 2401579.
[16] Z. M. Zhou, M. H. Sun, Y. B. Zhu, P. Z. Li, Y. R. Zhang, M. K. Wang, Y. Shen, A thioether-decorated triazine-based covalent organic framework towards overall H_2O_2 photosynthesis without sacrificial agents, Appl. Catal. B Environ. 334 (2023) 122862.
[17] M. P. Kou, Y. Y. Wang, Y. X. Xu, L. Q. Ye, Y. P. Huang, B. H. Jia, H. Li, J. Q. Ren, Y. Deng, J. H. Chen, Y. Zhou, K. Lei, L. Wang, W. Liu, H. W. Huang, T. Y. Ma, Molecularly Engineered Covalent Organic Frameworks for Hydrogen Peroxide Photosynthesis, Angew. Chem. Int. Ed. 61 (2022) e202200413.
[18] F. Y. Liu, P. Zhou, Y. H. Hou, H. Tan, Y. Liang, J. L. Liang, Q. Zhang, S. J. Guo, M. P. Tong, J. R. Ni, Covalent organic frameworks for direct photosynthesis of hydrogen peroxide from water, air and sunlight, Nat. Commun. 14 (2023) 4344.
[19] X. C. Zhang, J. Z. Zhang, J. Miao, X. Wen, C. Chen, B. X. Zhou, M. C. Long, Keto-enamine-based covalent organic framework with controllable anthraquinone moieties for superior H_2O_2 photosynthesis from O2 and water, Chem. Eng. J. 466 (2023) 143085.
[20] Y. Mou, X. D. Wu, C. C. Qin, J. Y. Chen, Y. L. Zhao, L. B. Jiang, C. Zhang, X. Z. Yuan, E. H. Ang, H. Wang, Linkage Microenvironment of Azoles-Related Covalent Organic Frameworks Precisely Regulates Photocatalytic Generation of Hydrogen Peroxide, Angew. Chem. Int. Ed. 62 (2023) e202309480.